Molecular Modelling of the Interaction of Cyanoacrylate Inhibitors with Photosystem II
Part 2. The Effect of Stereochemistry of Inhibitor Binding

Simon P. Mackay and Patrick J. O'Malley
Department of Chemistry, Sackville Street, UMIST, Manchester, M 60 1 QD, U.K.

Z. Naturforsch. **48c,** 782–787 (1993); received February 22/June 3, 1993

Cyanoacrylate Inhibitors, Photosystem II, Stereochemistry

The 2-cyanoacrylate inhibitors are a potent class of herbicides which block electron transfer in photosystem II. The spatial arrangement of different functional groups are an important factor in determining activity and a number of derivatives have been used as stereospecific probes of the secondary quinone binding site. More than one region of stereoselectivity in the binding site has been identified which influences the interaction with specific groups of the inhibitor. We have studied the interaction of various stereoisomers of the cyanoacrylates with the binding site in the D 1 protein (residues Leu 210 to Val 280) by determining the nonbonded intermolecular energies between the modelled structures calculated by van der Waals and electrostatic interactions after energy minimization of the combined structures to reduce inter and intramolecular strain and have found that the results reflect the experimentally determined data.

Introduction

The reaction centres of *Rhodobacter sphaeroides* and *Rhodopseudomonas viridis* are mechanistically analogues of photosystem II (PS II) in higher plant chloroplasts [1]. In both PS II and the bacterial reaction centres, a photon of light causes the oxidation of a special reaction centre chlorophyll, with the resultant transfer of an electron to a tightly bound quinone (Q_A) which is then oxidized by a secondary quinone (Q_B) to form a stable semiquinone Q_B^-. A second photoreduction results in a second electron transfer to Q_B producing a fully reduced quinol which diffuses away from the reaction centre. Photosynthetic electron transport (PET) inhibitors such as the triazines, phenylureas and cyanoacrylates are believed to block electron transfer from Q_A to Q_B in PS II by displacing the secondary quinone from its binding site. Knowledge of the herbicide and Q_B binding site of the PS II reaction centre is important for the design of new herbicides and for the generation of herbicide resistant plants by molecular biologists. In the absence of high resolution crystal structures for PS II, molecular models have been constructed based upon functional and partial sequence homologies found between the L and M subunits of the photosynthetic bacteria and the PS II D 1 and D 2 proteins of higher plants [2–5]. In conjunction with hydropathy considerations, this has led to the proposal that the D 1 and D 2 proteins each consist of five hydrophobic helical spans through the photosynthetic membrane in a similar manner to the L and M subunits of the bacterial reaction centres [6, 7]. Studies by Sayre *et al.* [8] using antibiotics to map exposed segments add evidence to this proposed structure. Significantly, the Q_B and herbicide binding domains of the L and D 1 proteins located on and between the forth and fifth transmembrane helices, possess a number of conserved residues and molecular models of this region are structurally similar [2–5].

Previous attempts [9, 10] at modelling the interaction of herbicides with the Q_B site in the D 1 protein have been concerned with positioning the herbicide within the site to agree with the binding parameters determined from the bacterial data and mutation studies of the Q_B binding domain which affect the interaction [11–24]. Reliance simply on visualization could lead to very unfavourable steric interactions which are not apparent without quantification. Such studies also rely completely on hydrogen bonding interactions to position the herbicide in the site. Our studies suggest satisfaction of hydrophobic steric requirements are the more crucial. The interaction between PS II and the PET inhibitors has been studied extensively in terms of structure-activity relationships [25–28]

Reprint requests to Dr. S. P. Mackay.

Verlag der Zeitschrift für Naturforschung,
D-72072 Tübingen
0939–5075/93/0900–0782 $ 01.30/0

and have highlighted the importance of hydrophobicity as a prime determinant of inhibitory activity. The spatial arrangement of the different groups in the inhibitor molecule is crucial in determining activity suggesting a very precise orientation of the more potent inhibitors in the binding site. The binding site is also sensitive to stereochemical influences in inhibitor design and studies of these interactions would be useful for revealing the topography of the receptor.

The incorporation of an optically active α-methylbenzyl moiety into triazine and phenylurea herbicides revealed that the PS II receptor was able to discriminate between the enantiomers, with the *S*-isomer being the more active [29–32]. The optically active 3-α-methylbenzylamino cyanoacrylates also have different levels of activity, the *S*-isomer again being the more active enantiomer [33–36]. However, this can be reversed when a chiral centre is introduced elsewhere in the molecule, for example in the ether substituent [29]. In this instance, the *R*-isomer is the more active compound. In an attempt to understand these differences in activity, we have evaluated the nonbonded energy between the herbicide and the Q_B site to determine the optimum orientation in the PS II D1 protein based on the enthalpy of binding. The intermolecular energies between the herbicide and individual amino acids have been calculated to identify those residues involved in stereoselective binding.

Methods

The source of the parameters used to calculate nonbonded energies is the forcefield which is the empirical fit to the potential energy surface of the molecules involved. It defines the coordinates used, the mathematical form of the equations involving the coordinates and the parameters adjusted in the empirical fit of the potential energy surface [37, 38]. The forcefield employs a combination of internal coordinates (bond distances, angles and torsions) to describe the bonded part of the potential energy surface, and interatomic distances to describe the van der Waals and electrostatic interactions between atoms. For the purpose of calculating the intermolecular energies between the atoms of two molecules, we are interested in the expressions which determine the nonbonded interaction [39, 40].

The nonbonded van der Waals interaction are represented by the first two terms in Eqn. (1) where A_{ij} and B_{ij} are parameters with units of kcal mol^{-1} $angstrom^{-12}$ and kcal mol^{-1} $angstrom^{-6}$ respectively and R_{ij} is the distance between the atoms i and j in angstroms. The second component of the nonbonded intermolecular energy is the electrostatic energy, which is represented by the third expression in Eqn. (1) where q_i and q_j are the charges on atoms i and j and D is the dielectric constant. The intermolecular energy is computed by summing the energy contributions between atoms of the two molecules. The contribution between atoms interacting with atoms in the same molecule is ignored.

$$E_{\text{interaction}} = \sum_i \sum_j \frac{A_{ij}}{R^{12}_{ij}} - \frac{B_{ij}}{R^{6}_{ij}} + \frac{q_i q_j}{D R_{ij}} . \quad (1)$$

Enclosure analysis focuses on a smaller region of a molecular system in order to generate intermolecular energies between a ligand and individual amino acid residues within its binding site. In doing so, Eqn. (1) is used to calculate the interaction energy between the atoms of the ligand and the atoms of the residues which fall into a defined sphere of a given radius around that ligand. This allows the identification of the main residue-ligand nonbonded interactions which make up the intermolecular energy between the two molecules.

The model used was the D1 protein from the PS II photosynthetic reaction centre of *Pisum sativum* (coordinates supplied by J. H. A. Nugent, University College London). The Q_B binding domain was represented by residues Leu 210 to Val 280 and all other residues were deleted from the model for simplification. All hydrogen atoms, polar and non-polar were included. The model of the cyanoacrylate (**1**) was built from the atomic coordinates for the non-hydrogen atoms determined by X-ray crystallography [41] using the crystal building facility in the *CERIUS* molecular graphics program (Version 3.1, Molecular Simulations Ltd., Cambridge, U.K.). The hydrogen atoms were subsequently added and minimized accordingly. Atom partial charges and potentials for both protein and herbicide models were assigned according to the parameters defined within the Consistent Valence Force Field (CVFF) used by the *Discover* (Version 2.8.0) molecular simulation program to be used in conjunction with the *Insight II* (Version

2.1.0) molecular graphics modelling program (Biosym Technologies, San Diego, California). The herbicide was modified according to the functional group substitutions in compounds **2–5** and docked into the protein according to the coordinates determined for compound **1** and the β-substituent rotated by −100° relative to the crystal structure. Energy minimization of the combined structures involved constraining all heavy atoms to relieve unfavourable interactions between the protein and herbicide hydrogen atoms whilst maintaining the coordinates of the heavy atoms determined for the interaction in the original paper [42]. Energy minimization was performed using steepest descents and conjugate gradients algorithms successively until the average first derivative was less than 0.005 kcal mol^{-1} $angstrom^{-1}$. The cancellation of the nonbonded interactions between atoms after a specified cutoff distance was not carried out during minimization in order to achieve a more accurate final structure. A dielectric constant of one was employed throughout the study. A sphere of 8 angstrom radius around each functional group of the cyanoacrylate was used to calculate the nonbonded interaction energy between the herbicide and individual amino acid residues of the binding site.

Results and Discussion

We have previously demonstrated that the β-*iso*-propyl substituent of compound **1** required rotation by −100° from the crystal structure in order to minimize repulsion from the Ala 251 and Asn 267 residues within the β-group binding pocket which in turn aided in the alignment of the aralkyl group within its binding niche [42]. We proposed that this was due to mutual repulsion between the hydrogens of the methylene group of the aralkyl substituent and the α-methyl group of the β-substituent. The repulsive energy generated by this orientation was compensated by the substantial improvement in binding energy between the herbicide and the protein. The interaction between stereoisomeric derivatives of the cyanoacrylates and the binding site substantiates this theory. The enantiomers possessing a chiral α-methylbenzyl aralkyl moiety (**2** and **3**) have different inhibitory activities [33–36], the *S*-isomer being the more potent.

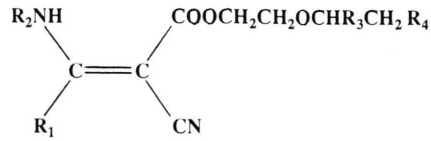

Compound	R_1	R_2	R_3	R_4
1	CH_3CHCH_3	(−)*p*-$ClC_6H_4CH_2$	H	H
2	CH_3CHCH_3	(*S*)*p*-$ClC_6H_4CH(CH_3)$	H	H
3	CH_3CHCH_3	(*R*)*p*-$ClC_6H_4CH(CH_3)$	H	H
4	CH_3CHCH_3	(−)*p*-$ClC_6H_4CH_2$	(*S*) CH_3	CH_3
5	CH_3CHCH_3	(−)*p*-$ClC_6H_4CH_2$	(*R*) CH_3	CH_3

In the *S* configuration, the methyl of the *iso*-propyl β-substituent and the chiral α-methyl are *trans* with respect to the enoate plane (Fig. 1) when the β-substituent is in the rotated conformation. This minimizes the mutual repulsion between the methyl functions but a repulsive energy of +11.2 kcal mol^{-1} with the chiral hydrogen is still evident. As with the non-chiral compound **1** this ensures that the aralkyl substituent is orientated within its hydrophobic binding niche and the β-substituent is tightly bound within its highly restrained pocket formed by the Ala 251 and Asn 267 residues (Fig. 2). The net improvement in the intermolecular binding energy (−57.5 kcal mol^{-1}) offsets the repulsive energy between the two functional groups of the inhibitor. In an earlier study we have found that the hydrophobic pocket enclosed by the aromatic residues Phe 211, Phe 255, Tyr 262, Tyr 265 and Phe 274 confers stereoselectivity on the *S*-isomer of the α-methylbenzyl derivative of atrazine [43]. It may be significant that this is the

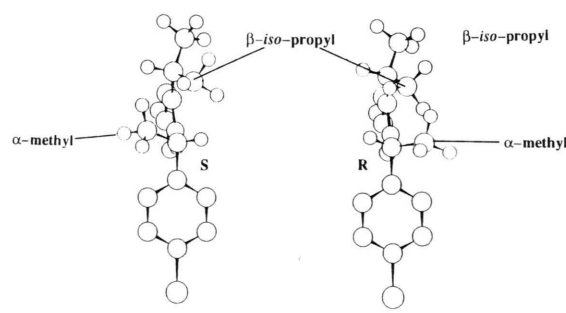

Fig. 1. The relative positioning of the β-substituent with respect to the chiral methyl group. The *S*-conformation shows a *trans* arrangement of the methyl and α-methyl (of the β-*iso*-propyl group) and the *R*-conformation a *cis* arrangement.

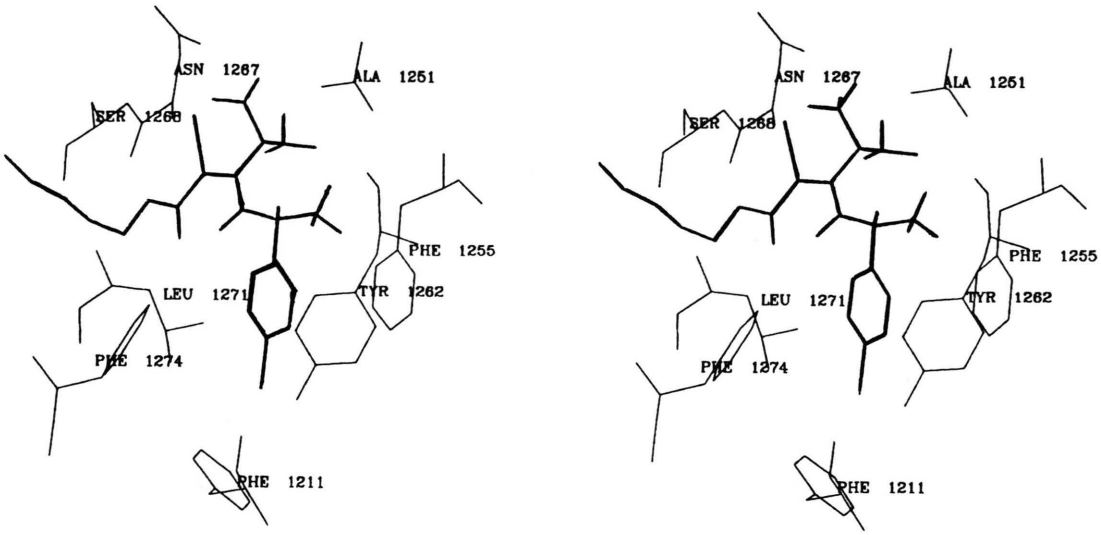

Fig. 2. Stereo plot of the binding of cyanoacrylate derivative **2** to the D 1 protein model of *Pisum sativum*. The β-ethyl substituent is rotated −100° compared to the crystal structure. The residue numbers of the D 1 protein are prefixed with the number 1. For viewing stereo plots a reflecting stereoscope (available from Aldrich) permits three dimensional perception.

same area of the receptor which binds the chiral phenyl substituent of cyanoacrylate **2.**

The chiral methyl group occupies a hydrophobic pocket within the receptor enclosed by the Ala 251, Leu 218 and Phe 255 residues. It has been recognized that discrimination between the two enantiomers could be due to two possibilities. Firstly, when the cyanoacrylate binds to the protein, the α-methyl substituent could be repulsed by an amino acid residue within the receptor when in the *R*- but not the *S*-configuration. Alternatively, the α-methyl group in both configurations could interact with the same binding pocket but this, by differentially affecting the spatial configuration of other structural elements in the molecule relative to the receptor, could lead to one enantiomer being favoured over another. We propose that discriminatory binding can be explained more easily by the latter theory. Inversion of the chiral methyl and hydrogen to produce the *R*-isomer **3** in the same binding orientation with the receptor as **2** produces an intermolecular binding energy of −52.1 kcal mol^{-1}. There is a repulsive interaction between the chiral methyl group and the Asn 266 residue (4.11 kcal mol^{-1}) but this is not significantly greater than the repulsion with the Phe 255 residue when in the *S* conformation (3.3 kcal mol^{-1}). However, there is a large intramolecular repulsive energy between the chiral methyl group and the methyl of the β-*iso*-propyl substituent of 353.4 kcal mol^{-1} which makes this *cis* conformation with respect to the enoate plane (Fig. 1) an unlikely possibility. Consequently, the β-substituent is rotated to reduce this repulsive force. Binding energy is therefore a balance between the inherent energy of the inhibitor's own conformation and the interaction with the receptor. Fig. 3 demonstrates this relationship. The configuration of the β-*iso*-propyl group according to the coordinates from the crystal structure (represented by an of angle 0°) has a minimum intramolecular repulsive energy of 5.6 kcal mol^{-1} with the chiral methyl group. The corresponding intermolecular energy with the receptor is −18.0 kcal mol^{-1} which deteriorates rapidly as the β substituent is rotated within its highly restrained pocket and is repulsed by the Ala 251 residue. The intermolecular energy improves after a maximum at −40° but at this stage the intramolecular repulsive energy begins to rise. Overall, the minimum energy interactive structure is achieved when the β-group adopts the crystal conformation. The alternative reorientation of the aralkyl moiety to minimize repulsions with the *iso*-propyl group results in a structure which cannot be accomodated within the binding site architecture according to our model. We therefore conclude

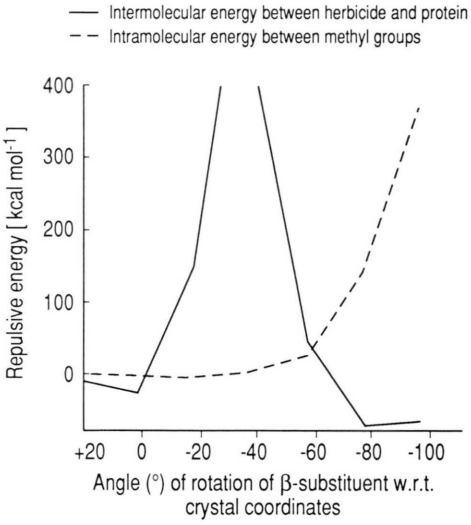

Fig. 3. Schematic representation of the relationship between the methyl–methyl repulsive energy within the inhibitor **3** and the intermolecular binding energy with the protein.

that the α-methyl group in both configurations acts to differentially affect the spatial configuration of the β-substituent in the molecule relative to the receptor, which leads to the *S*-isomer being favoured over the *R*-isomer.

We have also investigated a reported second stereoselective region of the receptor which is involved in binding the ethoxyether substituent of the cyanoacrylates. Here, the discrimination is against the *S*-isomeric form of a terminal *sec*-butoxy group **4.** Although the hydrogen bond between the ether oxygen and the Ser 268 hydroxyl side chain can be maintained, the chiral ethyl substituent is in direct conflict with the Glu 231 (33.8 kcal mol^{-1}) and the His 272 (6.2 kcal mol^{-1}) residues when in the *S*-conformation producing a relatively poor binding energy of −13.3 kcal mol^{-1}. In the *R*-conformation **5,** the smaller methyl group occupies the niche enclosed by the same two residues which improves the interaction energy with each to −0.7 kcal mol^{-1} producing a total intermolecular energy of −52.0 kcal mol^{-1} (Fig. 4). The

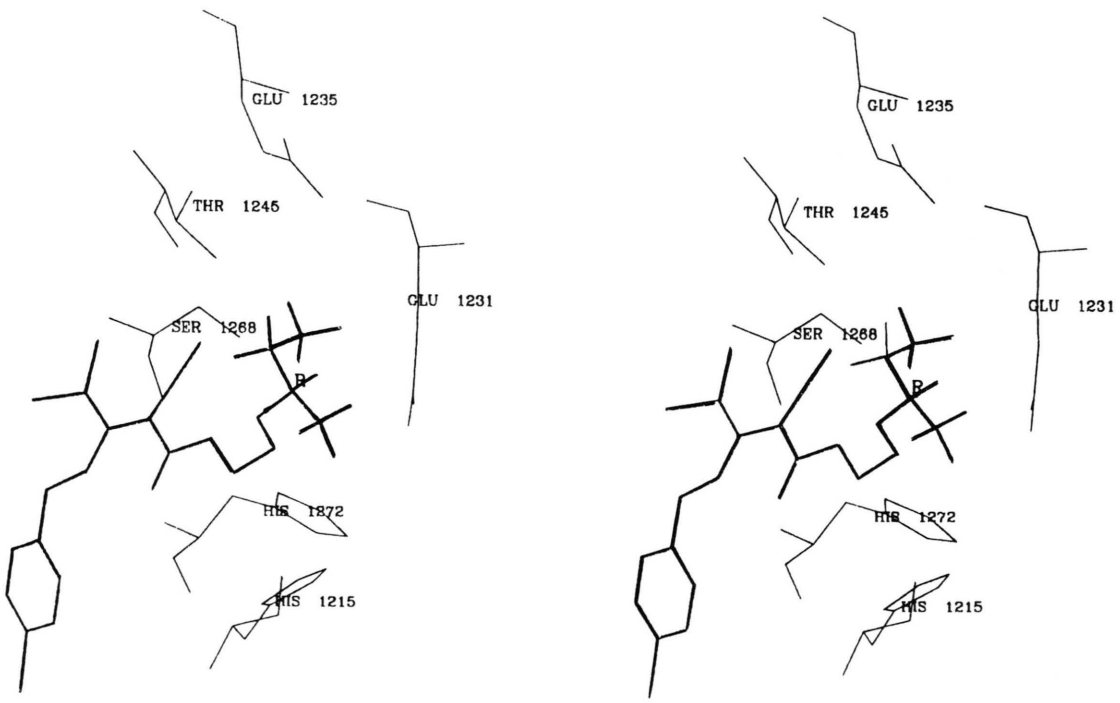

Fig. 4. Stereo plot of the binding of cyanoacrylate derivative **5** to the D1 protein model of *Pisum sativum.* The ethyl substituent is moved out of direct conflict with the Glu 231 and His 272 residues. The residue numbers of the D1 protein are prefixed with the number 1.

differential binding activity between isomers can be explained in terms of a direct stereoselective interaction between the protein and the groups around the chiral carbon.

It appears therefore that stereoselective binding is a complex process which can arise from conformational changes to the inhibitor induced by the topography of the receptor (at the β-group binding pocket) as an indirect consequence of chirality, or by the direct interaction between two chiral regions, one in the receptor, the other in the inhibitor (the ether binding pocket).

Acknowledgements

We thank the AFRC and the Royal Society for their support of this work. We acknowledge S. V. Ruffle and J. H. A. Nugent for the coordinates of PS II.

[1] C. Wraight, in: Photosynthesis: Energy Conversion by Plants and Bacteria (Govindjee, ed.), Vol. **1,** pp. 17–61, Academic Press, New York 1982.
[2] A. Trebst, Z. Naturforsch. **40c,** 237–241 (1985).
[3] A. Trebst, Z. Naturforsch. **42c,** 742–750 (1987).
[4] B. Svensson, I. Vass, E. Cedegren, and S. Styring, EMBO J. **9,** 2051–2059 (1990).
[5] S. Ruffle, D. Donnelly, T. Blundell, and J. Nugent, Photosynth. Res. **34,** 287–300 (1992).
[6] H. Michel, K. Weyer, H. Gruenberg, I. Dunger, D. Oesterhelt, and F. Lottspeich, EMBO J. **5,** 1149–1158 (1986).
[7] A. Trebst, Z. Naturforsch. **41c,** 240–245 (1986).
[8] R. Sayre, B. Andersson, and L. Bogorad, Cell **47,** 601–608 (1986).
[9] J. Bowyer, M. Hilton, J. Whitelegge, P. Jewess, P. Camilleri, A. Crofts, and H. Robinson, Z. Naturforsch. **45c,** 379–387 (1990).
[10] K. Tietjen, J. Kluth, R. Andree, M. Haug, M. Lindig, K. Miller, H. Wroblowsky, and A. Trebst, Pestic. Sci. **31,** 65–72 (1991).
[11] H. Michel, O. Epp, and J. Deisenhofer, EMBO J. **5,** 2445–2451 (1986).
[12] I. Sinning, H. Michel, P. Mathis, and A. W. Rutherford, Biochemistry **28,** 5544–5553 (1989).
[13] I. Sinning, J. Koepke, B. Schiller, and H. Michel, Z. Naturforsch. **45c,** 455–458 (1990).
[14] I. Sinning, J. Koepke, and H. Michel, in: Springer Series in Biophysics, Reaction Centres of Photosynthetic Bacteria (M. E. Michelle-Beyerle, ed.), Vol. **6,** pp. 199–208, Springer Verlag 1990.
[15] I. Sinning, TIBS **17,** 150–154 (1992).
[16] U. Johanningmeier, U. Bodner, and G. F. Wildner, FEBS Lett. **211,** 221–224 (1987).
[17] F. Sato, Y. Shigematsu, and Y. Yamada, Mol. Gen. Genet. **214,** 358–360 (1988).
[18] J. M. Erickson, M. Rahire, J.-D. Rochaix, and L. Mets, Science **228,** 204–207 (1985).
[19] S. S. Golden and R. Haselkorn, Science **229,** 1104–1107 (1985).
[20] G. Ajlani, D. Kirilovsky, M. Picaud, and C. Astier, Plant Mol. Biol. **13,** 469–480 (1989).
[21] J. C. Gingrich, J. S. Buzby, V. L. Stirewalt, and D. A. Bryant, Photosynth. Res. **16,** 83–89 (1988).
[22] N. Ohad and J. Hirschberg, Photosynth. Res. **23,** 73–79 (1990).
[23] N. Ohad and J. Hirschberg, Plant Cell **4,** 273–282 (1992).
[24] A. Aiach, Z. Naturforsch. **47c,** 245–248 (1992).
[25] K. Mitsutake, H. Iwamura, R. Shimizu, and T. Fujita, J. Agric. Food Chem. **34,** 725–732 (1986).
[26] S. Creuzet, B. Gilquin, and J. M. Ducruet, Z. Naturforsch. **44c,** 435–443 (1989).
[27] A. Trebst, W. Donner, and W. Draber, Z. Naturforsch. **39c,** 405–411 (1984).
[28] E. Kakkis, V. C. Palmire, C. D. Strong, W. Bertsch, C. Hansch, and U. Schirmer, J. Agric. Food Chem. **32,** 133–144 (1984).
[29] J. N. Phillips, in: Chemicals in Agriculture, Stereoselectivity of Pesticides (E. Ariens, ed.), Vol. **1,** pp. 183–220, Elsevier 1988.
[30] G. Gardner and J. Sanborn, Z. Naturforsch. **42c,** 663–669 (1987).
[31] R. Shimizu, H. Iwamura, and T. Fujita, J. Agric. Food Chem. **36,** 1276–1280 (1988).
[32] H. Omakawa and M. Konnai, Agric. Biol. Chem. **54,** 2373 (1990).
[33] J. N. Phillips and J. L. Huppatz, Z. Naturforsch. **42c,** 674–678 (1987).
[34] J. N. Phillips and J. L. Huppatz, Z. Naturforsch. **42c,** 679–683 (1987).
[35] J. N. Phillips and J. L. Huppatz, Z. Naturforsch. **42c,** 670–673 (1987).
[36] J. N. Phillips and J. L. Huppatz, Z. Naturforsch. **42c,** 684–689 (1987).
[37] A. T. Hagler, P. Dauber, and S. Lifson, J. Am. Chem. Soc. **101,** 5122–5130 (1979).
[38] A. T. Hagler, P. S. Stern, R. Sharon, J. M. Becker, and F. Naider, J. Am. Chem. Soc. **101,** 6842–6852 (1979).
[39] A. D. Buckingham and B. D. Utting, Annu. Rev. Phys. Chem. **21,** 287 (1970).
[40] P. Clarerie, in: Intermolecular Interactions, p. 69, B. Pullman, Wiley Interscience, New York 1981.
[41] H. G. McFadden, D. C. Craig, J. L. Huppatz, and J. N. Phillips, Z. Naturforsch. **46c,** 93–98 (1991).
[42] S. P. Mackay and P. J. O'Malley, Z. Naturforsch. **48c,** 773–781 (1993).
[43] S. P. Mackay and P. J. O'Malley, Z. Naturforsch. **48c,** 474–481 (1993).